

Article

Analysis of the Impact of Split Injection on Fuel Consumption and NO_x Emissions of Marine Medium-Speed Diesel Engine

Vladimir Pelić ¹, Tomislav Mrakovčić ^{2,*}, Radoslav Radonja ¹ and Marko Valčić ²

¹ Faculty of Maritime Studies, University of Rijeka, Studentska ulica 2, 51000 Rijeka, Croatia; vpelic@pfri.hr (V.P.); radonja@pfri.hr (R.R.)

² Faculty of Engineering, University of Rijeka, Vukovarska 58, 51000 Rijeka, Croatia; mvalcic@riteh.hr

* Correspondence: tomlav.mrakovcic@riteh.hr; Tel.: +385-51-651-520

Received: 29 September 2020; Accepted: 16 October 2020; Published: 20 October 2020



Abstract: The medium-speed diesel engine in diesel-electric propulsion systems is increasingly used as the propulsion engine for liquefied natural gas (LNG) ships and passenger ships. The main advantage of such systems is high reliability, better maneuverability, greater ability to optimize and significant decreasing of the engine room volume. Marine propulsion systems are required to be as energy efficient as possible and to meet environmental protection standards. This paper analyzes the impact of split injection on fuel consumption and NO_x emissions of marine medium-speed diesel engines. For the needs of the research, a zero-dimensional, two-zone numerical model of a diesel engine was developed. Model based on the extended Zeldovich mechanism was applied to predict NO_x emissions. The validation of the numerical model was performed by comparing operating parameters of the basic engine with data from engine manufacturers and data from sea trials of a ship with diesel-electric propulsion. The applicability of the numerical model was confirmed by comparing the obtained values for pressure, temperature and fuel consumption. The operation of the engine that drives synchronous generator was simulated under stationary conditions for three operating points and nine injection schemes. The values obtained for fuel consumption and NO_x emissions for different fuel injection schemes indicate the possibility of a significant reduction in NO_x emissions but with a reduction in efficiency. The results showed that split injection with a smaller amount of pilot fuel injected and a smaller angle between the two injection allow a moderate reduction in NO_x emissions without a significant reduction in efficiency. The application of split injection schemes that allow significant reductions in NO_x emissions lead to a reduction in engine efficiency.

Keywords: marine diesel engine; split injection; fuel consumption; NO_x emissions

1. Introduction

Energy efficiency and environmental friendliness are the basic criteria when choosing the optimal technology in any industry, so this is also the case with the transport of goods. It is known that the transport of goods by sea is the most efficient mode of transport. Nevertheless, maritime transport is facing increasing demands on energy efficiency and the lowest possible environmental impact. The requirements for reducing air pollution with pollutants from marine power plants are defined in MARPOL 73/78 (International Convention for the Prevention of Pollution from Ships), Annex VI (Prevention of Air Pollution from Ships, enforced since 19 May 2005). For marine diesel engines with a rated power of more than 130 kW the NO_x emission limits are divided into Tier I, Tier II and Tier III according to the IMO (International Maritime Organization). The limit values are applied depending on engine power and speed, the date of construction and the area of navigation, as shown in Figure 1.

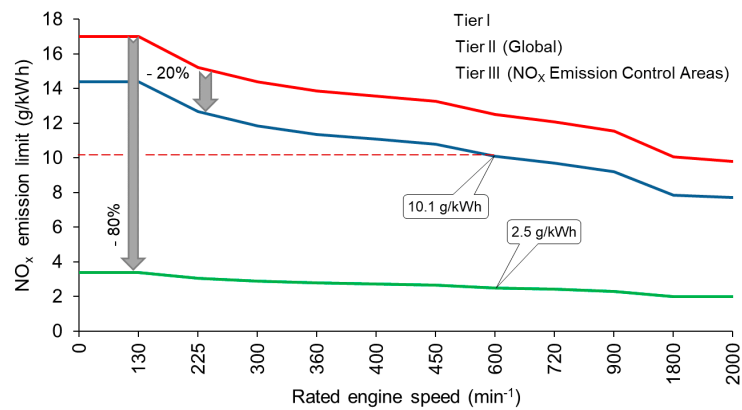


Figure 1. NO_x emission limits for marine engines [1].

Tier I refers to all ships built since 2000. Tier II is enforced since 2011. Due to the Tier II, the NO_x emission limits are reduced approximately 20% compared to Tier I. The Tier III requires approximately 80% reduction in emissions for ships operating in ECA (Emission Control Areas). Depending on their operating area of navigation, many ships are affected by Tiers II and III. It is therefore necessary to optimize the emissions of marine diesel engines. An example of determining the permissible NO_x emission for a marine diesel engine with a speed of 600 rpm is shown in Figure 1 by dashed red lines.

Most merchant ships are powered by a two-stroke low-speed diesel engine whose overall efficiency exceeds 50% under certain operating conditions. Marine medium-speed four-stroke diesel engines have approximately 3–5% lower efficiency than marine low-speed engines. Medium-speed diesel engines are half the size at the same rated power and NO_x emissions are considerably lower. The advantages of marine medium-speed diesel engines are especially pronounced if they are used in diesel-electric and hybrid propulsion systems. Slightly lower energy efficiency of four-stroke engines can be compensated by utilizing waste heat of the engine. This is supported by the fact that due to significantly higher exhaust gas temperatures of four-stroke engines, their exergy is significantly higher than that of two-stroke engines.

In marine diesel engines, various technologies are used to reduce emissions of harmful substances and in particular NO_x emissions, to the level required by regulations. These technologies usually are divided into primary and secondary measures. Primary measures involve modifying the process in the engine cylinder. Secondary measures include exhaust after treatment. Fuel type and quality also have a significant influence on emissions. Technologies for reducing NO_x emissions are listed in Table 1.

Table 1. NO_x emission reduction technologies [2].

No	NO _x Emission Reduction Technology	Expected Reduction
1	Two-stage turbocharging and Miller process	~40%
2	Combustion process adjustment	~10%
3	EGR—exhaust gas recirculation	~60%
4	Higher humidity of the scavenging air	~40%
5	Adding water to the fuel before injecting	~25%
6	Direct injection of water into the cylinder	~50%
7	SCR—selective catalytic reduction	~80%
8	Replacing liquid fuel with gaseous fuel	~85%

NO_x emission reduction technologies, which are marked 1, 2, 7 and 8 in Table 1, have the most favourable impact on energy efficiency and specific fuel oil consumption (SFOC). The implementation of other listed technologies leads to an increase in specific fuel consumption.

The adjustment of the combustion process in the engine cylinder by increasing the compression ratio while simultaneously reducing the amount of fuel injected per crankshaft revolution theoretically

enables the approximately constant pressure of the combustion process. This leads to a lower maximum pressure and a lower maximum temperature, which is beneficial because NO_x emissions are largely temperature-dependent. By using modern electronically controlled fuel injection systems, this technology does not lead to a significant increase in specific fuel consumption.

Numerical modelling of internal combustion engines is today an indispensable tool that speeds up the development of the engine while reducing development costs. The available literature offers different approaches to numerical modelling internal combustion engines. The target area of research, the required accuracy and the time available for calculations are the basic parameters for model selection [3–5]. Zero-dimensional single-zone models are an efficient tool for predicting motor performance in stationary and dynamic operating conditions using modest computing resources and fast performance of simulations [6–10]. Multi-zone combustion models [11–16] allow the prediction of emissions of NO_x and other pollutants such as soot. In addition to the mentioned advantage of multi-zone models, a longer calculation time is associated. These models are usually not suitable for determining the overall performance of engines and their energy balances but are mostly adapted to predict emissions. Rakopoulos et al. [17] described in detail the development and verification of a numerical model of a direct fuel injection diesel engine. The described model implies the division of the combustion space inside the cylinder into two zones. The chemical equilibrium method was used to calculate the concentration of individual pollutants in the exhaust gas. The development and application of a complex multi-zone model to simulate the operation of turbocharged diesel engines is described in Reference [18]. This model divides the fuel jet injected into the engine cylinder into a number of zones. The interaction of the jet with the cylinder walls, the influence of the injection angle and the conditions of fuel evaporation for each zone are taken into account. Scappin et al. [19] have successfully applied a zero-dimensional model with two zones for predicting NO_x emissions in electronically controlled low speed two-stroke marine diesel engine. A study of the impact of split fuel injection on diesel engines using the FIRE computer program is presented in Reference [20]. The paper investigates the influence of split fuel injection on the emission of solid particles and nitrogen oxides, using three different injection schemes. In Reference [21], the development and application of a zero-dimensional model with three zones for the analysis of the operating parameters of a high-speed diesel engine are presented. In Reference [22], a three-zone model is described that is applicable in real-time applications. Compared to other similar models, this study uses a procedure that does not require iterative resolution thus significantly shortening the computational time. Baldi et al. [23] presented a numerical model of a marine medium-speed diesel engine in which a zero-dimensional model is used to model the high-pressure part of the process while the mean value model is applied for the rest of process in the engine cylinder. More recently [24], the impact of multiple fuel injections on NO_x emissions has been investigated. Simulations show that by applying split injection it is possible to achieve a reduction in NO_x emissions without a significant increase in fuel consumption. The paper [25] describes the development of a semi-empirical multi-zone model for predicting nitrogen oxide emissions in high-speed diesel engines with direct fuel injection. As in most other papers, the extended Zeldovich mechanism of NO_x formation is applied here as well. The development of another semi-empirical model that allows good prediction of NO_x emissions under stationary operating conditions and engine loads is presented in Reference [26]. Model testing was performed on several diesel engines under different operating conditions and with simultaneous application of different methods to reduce NO_x emissions. While the research in these papers describes in detail different models of internal combustion engines to simulate nitrogen oxide emissions, few or no investigate the impact of split fuel injection with application to marine medium-speed diesel engines of 5000 kW and more.

The aim of this paper is to examine the impact of different split fuel injection schemes on the specific fuel consumption and nitrogen oxide emissions of a marine medium-speed diesel engine using a two zone combustion numerical model.

2. Numerical Model of a Four-Stroke Diesel Engine

The numerical model is based on the laws of conservation of energy and mass and solving the resulting differential equations described in References [6,27]. A one-zone, zero-dimensional model of the four-stroke diesel engine presented in Reference [28] was upgraded to two-zone model with possibility to predict NO_x emissions. The model has additional features such as variable integration step selection, variable inlet valve closing angle, adjustment of the turbocharger air mass flow and graphic display of the results.

The main advantages of the applied model compared to multidimensional and multi-zone models are lower complexity, higher execution speed, adaptability and satisfactory accuracy of the obtained results, which are comparable to more complex models.

An four-stroke diesel engine consists of the following interconnected subsystems (Figure 2): engine cylinder, inlet manifold, exhaust manifold, turbocharger, intercooler, fuel injection subsystem, piston mechanism and valve timing mechanism.

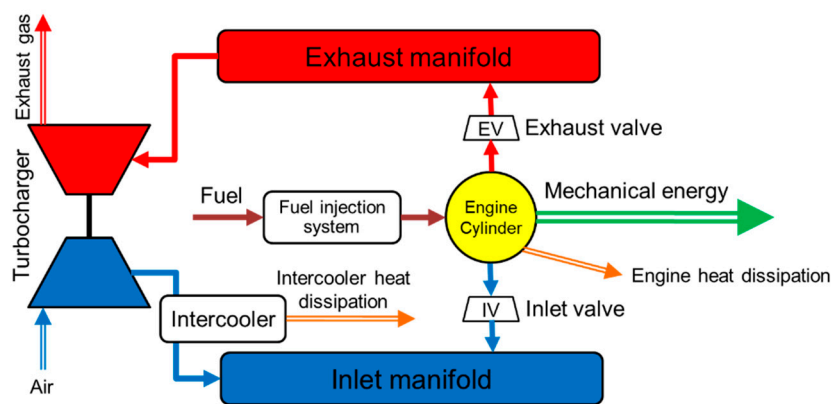


Figure 2. Diesel engine subsystems within implemented zero-dimensional numerical model.

The control volumes are interconnected by appropriate connections, which allow the exchange of the working medium. In the cylinder control volume, the heat is exchanged through the walls between the working medium and the cooling water. The heat is also exchanged with the ambient air through the walls of the inlet and outlet manifold. The heat generated by friction in the bearings is taken into account via the mechanical losses mean pressure, while the heat dissipated by radiation is neglected as it does not exceed 1% of the total heat input. Pressure and temperature in the control volumes are determined by solving differential equations derived from the laws of conservation of energy and mass. The properties of the working medium are determined according to References [29,30].

The software was developed in the C programming language. The model has been validated using data provided by the engine manufacturer and sea trial data. The data obtained from the operation of Wärtsilä 12V50DF engine on LNG ships with diesel-electric propulsion power systems. Rated power of one engine is 11.7 MW.

2.1. Mass Conservation Law

The mass change dm in the engine cylinder, inlet and exhaust manifold during the angle of rotation of the crankshaft $d\varphi$ is caused by the flow of the working medium through the inlet and exhaust valves, the mass of the injected fuel and the mass loss due to leakage can be expressed as:

$$\frac{dm_i}{d\varphi} = \frac{dm_{i,in}}{d\varphi} + \frac{dm_{i,ex}}{d\varphi} + \frac{dm_{i,f}}{d\varphi} + \frac{dm_{i,leak}}{d\varphi} \quad (1)$$

where m_{in} is the mass of the medium entering the control volume and m_{ex} is the mass of the medium exiting the volume, m_f is the mass of fuel supplied, m_{leak} is the mass of the medium exiting the volume

and subscript “i” denote control volume. If the engine is properly maintained the leaked mass from cylinder may be neglected.

2.2. Energy Conservation Law

Energy balance of the medium in the control volume is given by:

$$\frac{dQ_i}{d\varphi} = \frac{dQ_{i,f}}{d\varphi} + \frac{dQ_{i,w}}{d\varphi} + h_{in} \frac{dm_{i,in}}{d\varphi} + h_{ex} \frac{dm_{i,ex}}{d\varphi} + h_f \frac{dm_{i,f}}{d\varphi} - p \cdot dV \tag{2}$$

where $dQ_{i,f}$ denotes heat released through fuel combustion and $dQ_{i,w}$ heat exchanged through the walls. The variables h_{in} and h_{ex} represents the enthalpy of the medium entering or leaving the control volume and h_f is enthalpy of the fuel.

Assuming that the internal energy of the gas depends solely of temperature, the equation of the temperature change is given by

$$\frac{dT_i}{d\varphi} = \frac{1}{m_i \left(\frac{\partial u}{\partial T} \right)_i} \left[-p_i \frac{dV_i}{d\varphi} + \sum_j \frac{dQ_{i,j}}{d\varphi} + \sum_k h_{i,k} \frac{dm_{i,k}}{d\varphi} - u_i \frac{dm_i}{d\varphi} - m_i \left(\frac{\partial u}{\partial \lambda} \right)_i \frac{d\lambda_i}{d\varphi} \right] \tag{3}$$

where u_i denotes internal energy and λ is the equivalent ratio of air to fuel.

In previous equations, all variables containing the mass or enthalpy of the fuel refer only to the control volume in which the fuel burns or to the cylinder. The same applies to variables describing a change in volume. When the fuel burns in the cylinder, the chemical energy of the fuel is converted into heat, which increases pressure and temperature. The increased pressure acts on the piston, where the thermal energy is converted into mechanical work.

2.3. Indicated Work

Indicated mechanical work is determined by:

$$\frac{dW_c}{d\varphi} = p_c \frac{dV_c}{d\varphi} \tag{4}$$

The pressure p_c in the cylinder is determined using the equation of state for a gas:

$$p_c = \frac{m_c \cdot R_c \cdot T_c}{V_c} \tag{5}$$

Current cylinder volume V_c is derived from the crankshaft mechanism geometry:

$$V_c(\varphi) = \frac{V_s}{2} \left[(1 - \cos \varphi) + \frac{1}{\lambda_m} \left(1 - \sqrt{1 - \lambda_m^2 \sin^2 \varphi} \right) + \frac{2}{\varepsilon - 1} \right] \tag{6}$$

where V_s is the cylinder swept volume, ε is compression ratio and λ_m denotes ratio between crank radius and piston stroke.

2.4. Heat Exchange

Heat transfer through the cylinder walls can be expressed as:

$$\frac{dQ_{w,c}}{d\varphi} = \sum_i \alpha_c \cdot A_{w,c,i} (T_{w,i} - T_c) \frac{dt}{d\varphi} \tag{7}$$

According to References [31,32], there are no significant temperature changes under stationary operating conditions, therefore a mean cylinder wall temperature is assumed. Furthermore, relatively small deviations in the heat transfer coefficient can be neglected, so that the mean heat transfer

coefficient can be applied in the calculations. For the calculation of the heat transfer coefficient an empirical expression [33] is used in this paper:

$$\alpha_c = C_1 \cdot V_c^{-0.06} \cdot p_c^{0.8} \cdot T_c^{-0.4} \cdot (c_{mps} + C_2)^{0.8}, \tag{8}$$

where C_1 and C_2 are the empirical coefficients and c_{mps} is the mean piston speed.

2.5. Heat Release

Numerical models that describe the complex process of fuel combustion inside the cylinder is divided according to References [34,35] into zero-dimensional, quasi-dimensional and multidimensional models.

Vibe [36] provided the heat release rate by the following expression:

$$\frac{x_f}{d\varphi} = C (m + 1) \left(\frac{\varphi - \varphi_{IS}}{\varphi_{CD}} \right)^m \exp \left(-C \left(\frac{\varphi - \varphi_{IS}}{\varphi_{CD}} \right) \right)^{m+1} \tag{9}$$

where x_f is the relative portion of fuel burned, C is the constant that depends on the efficiency of fuel combustion. The subscript IS refers to the crankshaft angle at which ignition starts, while the subscript CD represents the duration of combustion. The exponent m is determined according to Reference [37] and the change in combustion duration $\Delta\varphi_{CD}$ is determined according to Reference [38].

The expressions for determining the ignition delay for diesel fuel are given in Reference [39]. Adjusted expression for heavy fuel are given in Reference [40].

It is assumed that the rate of injected fuel mass follows the heat release rate and that the combustion products are immediately mixed with the medium in the cylinder to form a homogeneous mixture. The total mass within the cylinder increases during combustion due to the injected fuel. The excess air in the engine cylinder is calculated from the mass of the gases in the engine cylinder and the mass of the injected fuel.

In the numerical sub-model of split fuel injection, a double Vibe function was used for pilot injection and a single Vibe function for main injection.

2.6. Change in Mass And Excess Air in The Cylinder

The change in mass in the engine cylinder due to fuel injection is expressed by:

$$\frac{dm_c}{d\varphi} = \frac{dm_{f,c}}{d\varphi} = \frac{dx_f}{d\varphi} m_{f,proc} = \frac{1}{\eta_{comb} LHV} \frac{dQ_f}{d\varphi} \tag{10}$$

Also, fuel injection affects the change in excess air ratio which is calculated as follows:

$$\frac{d\lambda_c}{d\varphi} = - \frac{\lambda_c}{m_{f,c}} \frac{dm_{f,c}}{d\varphi} \tag{11}$$

When the working medium flows out of the control volume, there is no change in the excess air ratio and there is no change in the gas composition. If gases flowing into the control volume have a different composition, there is also a change in the excess air ratio. The change in excess ratio as a function of the crankshaft angle is determined by the expression:

$$\frac{d\lambda_c}{d\varphi} = \frac{dm_{ci}}{d\varphi} \left(1 - \frac{\lambda_c S_{AFR} + 1}{\lambda_i S_{AFR} + 1} \right) \frac{1}{S_{AFR} m_{g,c}} \tag{12}$$

where S_{AFR} is stoichiometric mass of air in mixture with fuel.

2.7. Working Medium Exchange in A 4-Stroke Engine Cylinder

The working fluid flows between the cylinder and the inlet and exhaust manifolds. The flow of the working fluid from one control volume to the other is determined by valves timing, the effective flow area and the pressure difference:

$$\frac{dm}{d\varphi} = \alpha_p A_{p,geo} \psi p_1 \sqrt{\frac{2}{R_1 T_1}} \frac{dt}{d\varphi} \tag{13}$$

In the previous equation, the geometric flow areas $A_{p,geo}$ of the inlet and exhaust valves are determined according to the camshaft cam geometry. The flow coefficient α_p is determined according to Reference [41]. The flow function ψ for the subcritical pressure ratio is determined according to Reference [42]

$$\psi = \sqrt{\frac{\kappa}{\kappa - 1} \left[\left(\frac{p_2}{p_1} \right)^{\frac{2}{\kappa}} - \left(\frac{p_2}{p_1} \right)^{\frac{\kappa + 1}{\kappa}} \right]}, \text{ if } 1 \geq \frac{p_2}{p_1} \geq \left(\frac{2}{\kappa + 1} \right)^{\frac{\kappa}{\kappa + 1}} \tag{14}$$

and flow function ψ for supercritical pressure is:

$$\psi = \left(\frac{2}{\kappa + 1} \right)^{\frac{1}{\kappa - 1}} \sqrt{\frac{\kappa}{\kappa + 1}}, \text{ if } \frac{p_2}{p_1} < \left(\frac{2}{\kappa + 1} \right)^{\frac{\kappa}{\kappa + 1}} \tag{15}$$

Subscript 1 refers to the state in the upstream control volume, while subscript 2 refers to the state in the downstream control volume.

2.8. Turbocharger

For modelling the operation of a diesel engine under stationary operating conditions, the numerical model of the turbocharger does not require the use of suitable compressor map data. Instead, it is acceptable to assume that the air mass flow is known for a given engine load. Engine manufacturers typically provide inlet manifold pressure and air mass flow data for different engine loads in range between the 50% to 100% of engine MCR (Maximum Continuous Rating). The exhaust gases mass flow through the turbine is determined by the following expression:

$$\frac{dm_T}{d\varphi} = \alpha_T A_{T,geo} \psi p_{EM} \sqrt{\frac{2}{R_{EM} T_{EM}}} \frac{dt}{d\varphi} \tag{16}$$

where α_T is the flow coefficient, $A_{T,geo}$ denotes the cross-sectional area of the turbine, ψ is the flow function and p_{EM} is exhaust manifold pressure.

The temperature of the exhaust gases after the turbine is calculated according to:

$$T_{AT} = T_{EM} - \frac{|\Delta h_{T,is}|}{\eta_{T,is} \cdot c_{p,EG}} \tag{17}$$

2.9. Effective Engine Power

The indicated engine power is determined by integration of the total work of all cylinders during one duty cycle:

$$P_{ind} = \frac{n_M}{30 \tau} \sum_{i=1}^z \int \frac{dW_{C,i}}{d\varphi} d\varphi \tag{18}$$

where z denotes number of cylinders and n_M is crankshaft speed in rpm.

Effective engine power is calculated by the following equation:

$$P_{ef} = \frac{z n_M}{30 \tau} V_S p_{mep} = P_{ind} \frac{p_{mep}}{p_{mip}} \tag{19}$$

where P_{mep} is the mean effective pressure and P_{ind} is the mean indicated pressure. The mean effective pressure is determined by subtracting the mean pressure of the mechanical losses from the mean indicated pressure. The mean pressure of mechanical losses takes into account losses caused by friction and operation of oil and water pumps. In the developed numerical model, the mean pressure of mechanical losses is calculated using empirical expressions according to Reference [43].

For easier understanding and tracking of the interconnections between individual equations and submodels, the block diagram of the engine numerical model is shown in Figure 3.

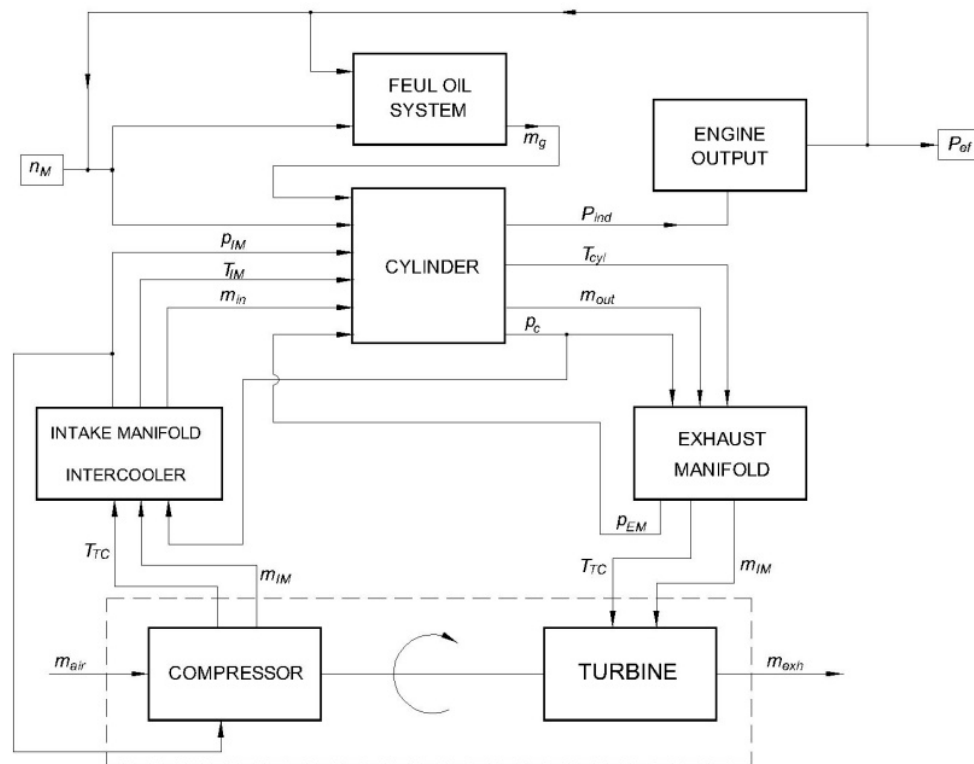


Figure 3. Block diagram of the engine numerical model.

3. Two-Zone Numerical Sub-Model

The formation of nitrogen oxides in the engine cylinder is exponentially dependent on the temperature at the boundary between the flame and the fresh medium in the cylinder. The formation of NO_x is exactly proportional to the available time in which the chemical reactions of formation and decomposition take place. Since the time in which the chemical reactions on which the formation of NO_x depends takes place is relatively short (depending on the engine speed), the process does not take place in conditions of chemical equilibrium.

The single-zone model only allows monitoring of the mean medium temperature in the engine cylinder. To predict the rate of NO_x formation with satisfactory accuracy, it is necessary to know the temperature at the boundary between the flame and the fresh medium in the engine cylinder. The following is a model in which during the part of the process in which the combustion and expansion of the working medium takes place, the control volume of the cylinder is divided into two zones. Such a model is also known in the literature as a quasi-dimensional combustion model and a detailed description of the two-zone model is presented in References [16,44,45].

In models with two or more zones, the formation of zones begins with the start of fuel combustion. After opening the exhaust valve, the process is observed as in models with single zone. Typically, a two-zone model divides the combustion space into a fresh medium zone and a zone made up of combustion products. The simplified model of the combustion process applied in this paper implies the division of the control volume of the engine cylinder into two zones:

- Zone 1—fresh mixture consisting of air, residual gases from the previous process and recirculated exhaust gases (only in case EGR is used), and
- Zone 2—combustion gases consisting of gaseous products of fuel combustion during stoichiometric combustion.

The model of the combustion process with two zones implies the following simplifications and assumptions:

- division of the working medium in the combustion space into two zones: the zone of fresh medium and the zone of combustion gases,
- the actual geometric shape of the zones is neglected and only their volume is taken into account,
- at the observed position of the crankshaft, the pressure in all zones is the same and does not depend on the position within the zone,
- at the observed position of the crankshaft, the temperature does not depend on the position within the zone and the same applies to the excess air,
- the working medium in each of the zones is a homogeneous mixture whose chemical composition and mass fractions of individual participants within the zone do not depend on the position within the zone,
- the formation of zones begins with the injection and combustion of fuel and until then there is only one zone,
- combustion in the combustion gas zone or in the edge layer (“flame front”) takes place in the conditions of a slightly “poor” mixture,
- there is no heat exchange between zones,
- heat exchange takes place only between Zone 2 (combustion gas zone) and the environment,
- at the moment of opening the exhaust valve, both zones are instantly mixed into a homogeneous mixture.

A schematic representation of the formation of zones and changes in the mass of the medium depending on the crankshaft angle φ for the process in a four-stroke diesel engine is given in Figure 4. The process begins with the suction stroke, whereby the mass of the medium in the cylinder increases. After closing the inlet valve, the mass of the medium in the cylinder does not change during the compression stroke until the moment of fuel injection into the engine cylinder.

The applied numerical model assumes that the pressure in individual zones is equal to the pressure in the cylinder and that it forms a homogeneous pressure field. Therefore, the values for the pressure are obtained by the calculation using the single-zone model.

$$p_C = p_1 = p_2 \quad (20)$$

Subscript “1” refers to Zone 1 (fresh medium zone) and subscript “2” to Zone 2 (combustion gas zone).

The mass of the medium in the cylinder is calculated according to:

$$m_C = m_1 + m_2 \quad (21)$$

After closing the inlet valve, the mass of the medium in the cylinder does not change until the fuel injection begins. The total mass of fresh medium in the cylinder is the sum of the masses: clean air, residual combustion gases and recirculated combustion gases.

$$m_C = m_1 = m_A + m_{RG} + m_{EGR} \tag{22}$$

Assuming that the combustion of fuel in the marginal layer (boundary between the zones) takes place with the prior mixing of the medium from Zone 1 with the injected fuel in a stoichiometric ratio, according to the expression:

$$\alpha_{st}^1 = \left(\frac{m_1}{m_f} \right)_{st} = \left(\frac{m_A + m_{RG} + m_{EGR}}{m_f} \right)_{st} \tag{23}$$

The mass of the medium in Zone 2 is determined from the known mass of burned fuel (data obtained from the single-zone model) and the stoichiometric ratio for Zone 1, according to the expression:

$$m_2 = m_f(1 + \alpha_{st}^1) \tag{24}$$

and the mass of the media in Zone 1 is calculated according to:

$$m_1 = (m_C + m_f) - [m_f(1 + \alpha_{st}^1)] = (m_A + m_{RG} + m_{EGR} + m_f) - m_2 \tag{25}$$

At any time or position of the crankshaft, the sum of the volumes of both zones is equal to the volume of the cylinder.

$$V_C = V_1 + V_2 \tag{26}$$

The volume of the zones is calculated using the equation of state of the ideal gas according to the expression:

$$V_i = \frac{m_i R_i T_i}{p_C} \tag{27}$$

Subscript "i" refers to the zone.

The temperature of the gases in Zone 1 is calculated according to the expression for the adiabatic change of state:

$$T_{1,k} = T_{1,k-1} \left(\frac{p_{C,k}}{p_{C,k-1}} \right)^{\frac{\kappa-1}{\kappa}} \tag{28}$$

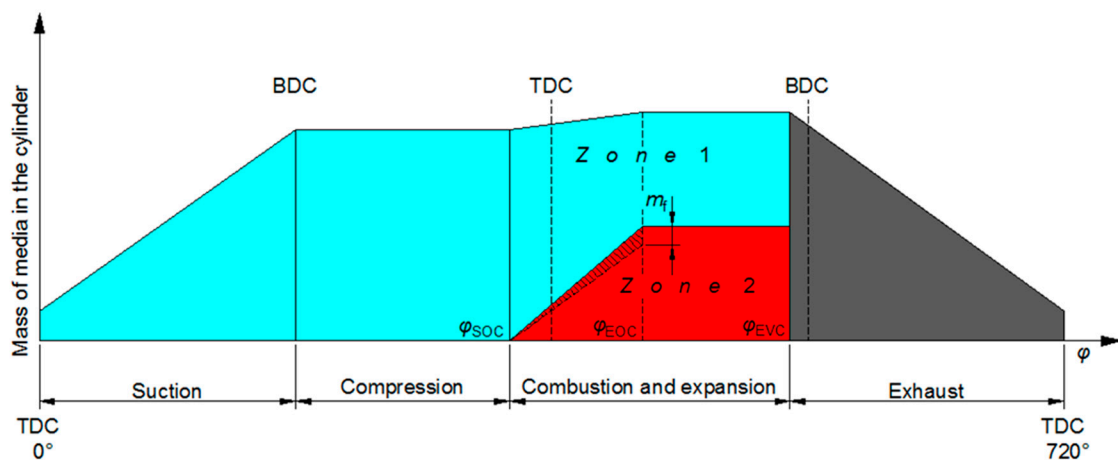


Figure 4. Formation of zones in the cylinder of a four-stroke diesel engine.

The subscript “k – 1” indicates the values of pressure and temperature from the previous calculation step.

The change in temperature in Zone 2 depending on the angle of the crankshaft is determined by applying the expression:

$$\frac{dT_2}{d\varphi} = \frac{1}{m_2 \left(\frac{\partial u}{\partial T}\right)_2} \left[\frac{dQ_f}{d\varphi} + \frac{dQ_w}{d\varphi} - p_c \frac{dV_2}{d\varphi} - u_2 \frac{dm_2}{d\varphi} + h_1 \frac{dm_2}{d\varphi} - m_2 \left(\frac{\partial u}{\partial \lambda}\right)_2 \frac{d\lambda_2}{d\varphi} \right] \quad (29)$$

where subscript 1 correspond to Zone 1 and subscript 2 to Zone 2, f represents fuel and w denote cylinder walls.

The changes in the mass and temperature of the medium in the zones depending on the position of the crankshaft obtained by applying the described numerical model are shown in Figures 5 and 6.

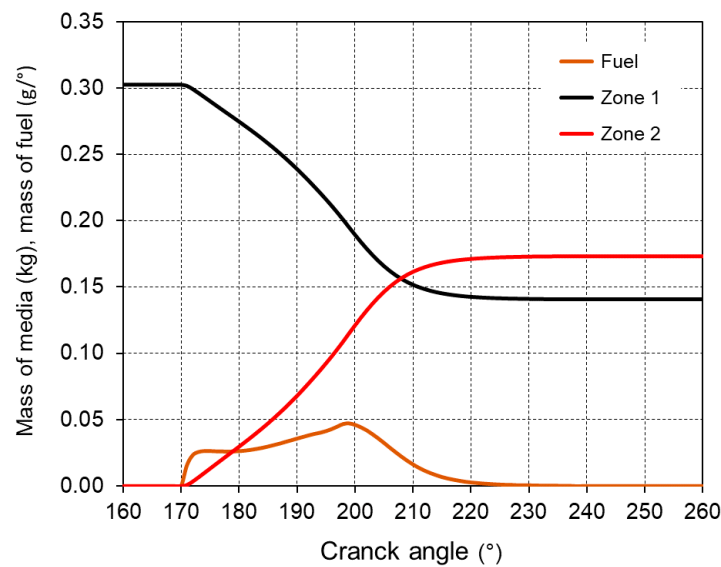


Figure 5. Change in mass of media in zones.

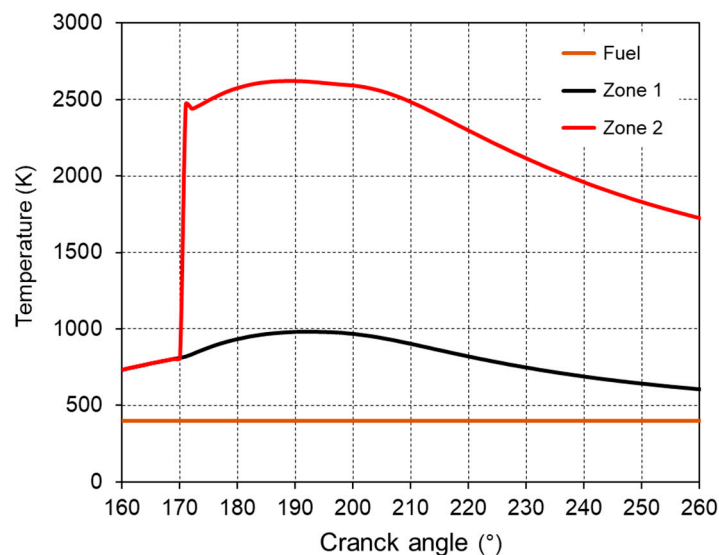


Figure 6. Change in temperature of media in zones.

4. Nitrogen Oxide Formation Submodel

The applied model of “thermal” nitrogen oxide formation is based on the extended Zeldovic mechanism. Models in which the formation of NO is described with three chemical reactions as

in papers [19,22,46] are most often used in the literature. Chemical reactions of formation and decomposition of nitrogen monoxide are:



In the conditions prevailing during combustion and due to the short time due to the relatively high speed of the combustion process, equilibrium concentrations of NO do not occur. All other chemical reactions that take place in the combustion space are assumed to take place at high speed and that the concentration of chemical elements and compounds (O₂, H, H₂, OH, N, N₂, CO, CO₂ and H₂O) is in a state of chemical equilibrium.

Changes in the concentration of NO in the chamber in which the combustion process takes place are calculated according to the expression:

$$\frac{d[\text{NO}]}{dt} = k_{1,f}[\text{O}]_e[\text{N}_2]_e - k_{1,d}[\text{NO}][\text{N}]_e + k_{2,f}[\text{N}]_e[\text{O}_2]_e - k_{2,d}[\text{NO}][\text{O}]_e + k_{3,f}[\text{N}]_e[\text{OH}]_e - k_{3,d}[\text{NO}][\text{H}]_e \tag{30}$$

The concentrations of all elements in square brackets marked with the subscript “e” are calculated from the chemical equilibrium conditions. The coefficients of formation rate $k_{i,f}$ and decomposition rates $k_{i,d}$ are calculated using the expressions from Reference [47].

Concentrations of individual components under the condition of chemical equilibrium, depending on pressure, temperature and equivalent ratio of fuel and air Φ are calculated using the model described in Reference [48]. In this model, diesel fuel was replaced by a hydrocarbon C₁₂H₂₆.

5. Validation of Numerical Model of the Engine

The developed numerical model of the engine was validated using the engine manufacturer data and measurements acquired during sea trial of LNG ships with diesel-electric propulsion.

Validation of numerical model of the engine was based on the Wärtsilä 12V50DF engine data (Table 2). All presented data refers to engine performance running on heavy fuel oil (HFO).

Table 2. Wärtsilä 12V50DF engine data [49].

Engine General Technical Data	Value/Type
Bore, mm	500
Stroke, mm	580
Valves per cylinder (inlet/exhaust)	2/2
Inlet/outlet valve diameter, mm	165/160
Number of cylinders and configuration	12 cylinders, V/45°
Maximum continuous rating (MCR), kW	11,700
Engine speed, rpm	514
Mean piston speed, m s ⁻¹	9.9
Number of turbochargers	2
Turbocharger type	ABB TPL71-C

Manufacturer’s records at different loads (Table 3) and sea trial records LNG carrier (Table 4) were compared with the results obtained by numerical simulations.

Table 3. Manufacturer’s data for Wärtsilä W 12V50 DF engine [49].

Engine Load	50%	75%	100%
Engine power, kW	5850	8775	11,700
Specific fuel oil consumption, g/kWh	196	187	189
Exhaust gas temperature after turbocharger, °C	337	336	352
Exhaust gas mass flow, kg/s	13.9	18.4	23.0

Table 4. Sea trial records for Wärtsilä 12V50 DF engine (sea trial).

Engine Load	40%	50%	71%
Engine power, kW	4680	5850	8307
Specific fuel oil consumption, g/kWh	199	197	190
Maximum cylinder pressure, bar	70	83	107
Exhaust gas temperature after turbocharger, °C	412	392	359

The simulation of engine operation under steady-state conditions was performed for five operating points in the range of 40% to 100% of the engine rated power. Model validation was performed by comparing data from Tables 3 and 4 with data obtained by simulating specific fuel consumption, maximum cylinder pressure, exhaust gas temperature and exhaust gas mass flow. Figure 7 shows closed indicating diagrams for five engine operating regimes obtained by developed engine operation simulation software.

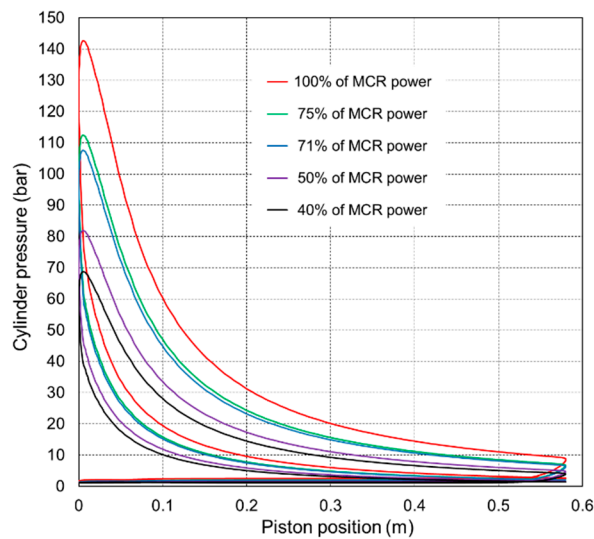


Figure 7. Closed indicated pressure diagrams at 40% to 100% of engine rated power.

Figure 8 shows the comparison of the specific fuel oil consumption measured on the test bed and during the sea trial with the values obtained by the engine simulation model. The largest deviation occurs at 40% of the engine load, which is approximately 3.5%, that is, 7 g/kWh. The smallest deviation from the measured data occurs between 50% and 71% of the maximum engine load and is less than 1%, that is, 2 g/kWh.

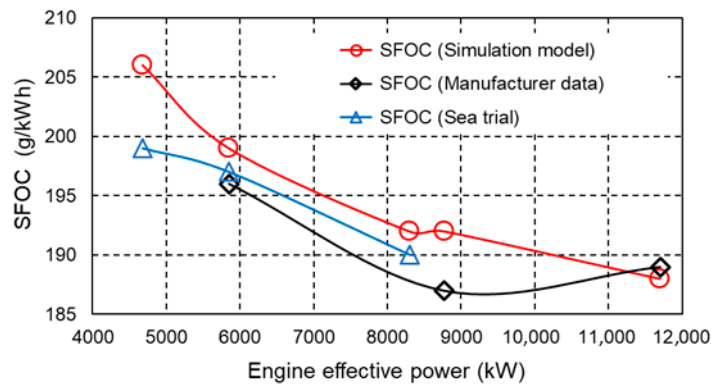


Figure 8. Comparison of the specific fuel oil consumption.

Figure 9 shows a comparison of the maximum pressures in the engine cylinder. The absolute pressure deviations are less than 1 bar at all observed operating regimes. The maximum pressure in the engine cylinder measured during the sea trial is presented as an average value of all 12 cylinders.

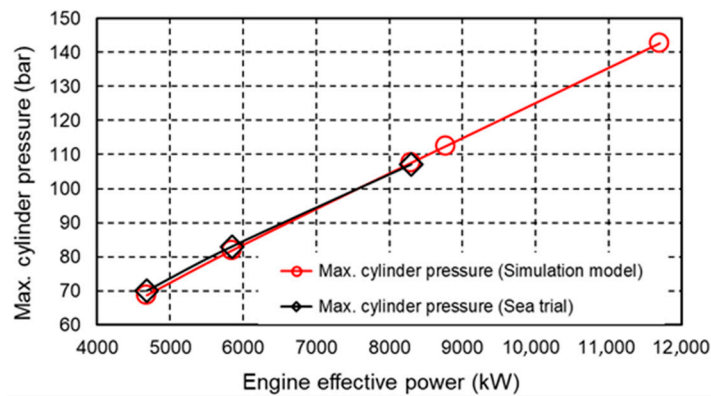


Figure 9. Comparison of maximum pressures in the engine cylinder.

Figure 10 shows the comparison of exhaust gas temperatures after the turbocharger. The biggest difference occurs at 50% of the engine load and its value is 10.4%, that is, 35 °C. The deviation at the same operating point compared to the sea trial data is 6.8%, that is, 20 °C. The difference between the exhaust gas temperatures after the turbocharger is only 1.7%, that is, 6 °C at full engine load.

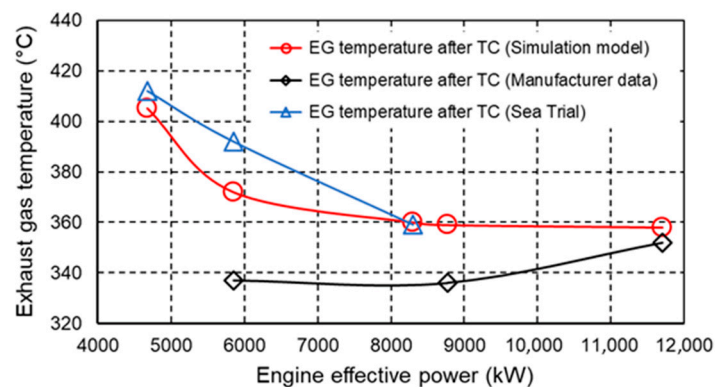


Figure 10. Comparison of the exhaust gas temperatures after turbocharger.

Comparison of the exhaust gas mass flows shown in Figure 11 indicate on very small deviations between manufacturer’s data and results obtained by numerical model of the engine.

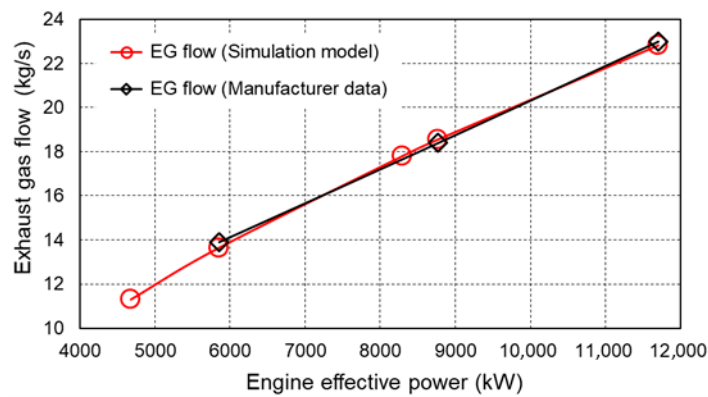


Figure 11. Comparison of exhaust gas mass flows.

6. Split Fuel Injection Impact on SFOC and NO_x Emission

Split fuel injection can be used as a method to reduce NO_x emissions during combustion due to decreasing of temperature and pressure in the cylinder. The process in the diesel engine cylinder from the beginning of the fuel injection to the end of the fuel combustion takes place in four phases, as shown in Figure 12. The first phase (1) is called the ignition delay and it involves the evaporation and mixing of the fuel until the conditions for ignition of the resulting fuel mixture are met. The second phase (2) is characterized by the relatively intensive combustion of the fuel mixture formed during the ignition delay period. The second phase is called the combustion of the previously formed mixture (premixed burning) and there is an intense release of heat which causes a sudden rise in temperature and pressure in the cylinder. After the initial sharp increase in the heat release rate, a third phase (3) follows in which the combustion rate is controlled by the rate of mixing of the remaining fuel with the fresh medium. In the third phase, called mixing controlled combustion, the heat release rate is lower than in the previous phase. During the fourth phase (4) of combustion, the remaining fuel burns out and this phase is called late combustion.

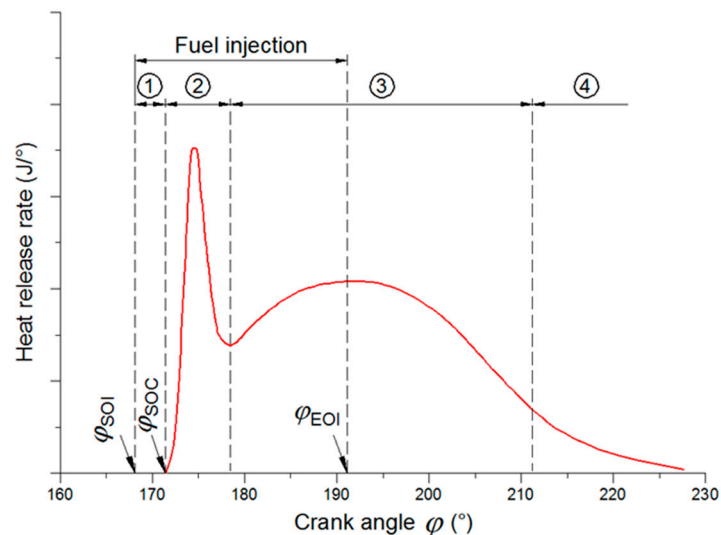


Figure 12. Heat release rate and phase of combustion process.

The use of split injection can significantly affect the course of the combustion process or the amount of harmful substances in the exhaust gases of diesel engines. Pilot injection has a significant impact on the reduction of NO_x emissions as well as noise generated during the combustion. While subsequent fuel injection can achieve a reduction in soot emissions, as well as an increase in the exhaust gas

temperature required when applying secondary exhaust aftertreatment measures. The basic principle of split fuel injection into the engine cylinder is shown in Figure 13.

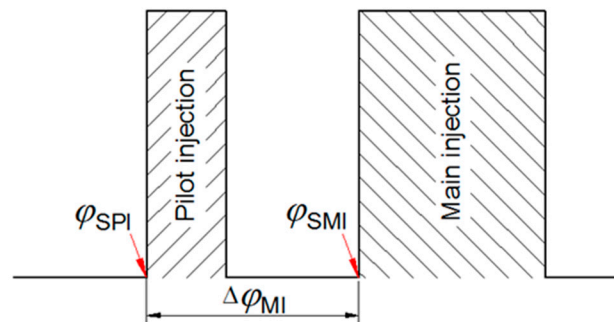


Figure 13. The basic principle of split fuel injection.

In Figure 13, the following labels were used:

φ_{SPI} —start of pilot injection,

φ_{SMI} —start of the main injection,

$\Delta\varphi_{MI} = \varphi_{SMI} - \varphi_{SPI}$.

If applying an appropriate split injection scheme, it is possible to effectively control emissions. However, the attention has to be paid to the specific fuel consumption. It is necessary to choose an injection scheme in which a compromise will be reached between reducing emissions and increasing specific fuel consumption.

The results of experimental research [50–52] have shown that increasing the amount of pilot injected fuel increases NO_x emissions, while increasing the difference $\Delta\varphi_{MI}$ between the pilot and the main injection leads to an increase in specific fuel consumption.

In this study, the analysis of split injection was performed for stationary engine operating conditions at 50%, 75% and 100% of the rated engine power. For research purpose, nine schemes of fuel injection were selected.

For all three load cases, engine operation was simulated with 10%, 20% and 30% of pilot injection for total amount of fuel injected. Difference $\Delta\varphi_{MI}$ was varied as 3, 6 and 9 degrees of crankshaft angle for each pilot injection.

The corresponding injection schemes (Schemes 1–9) are marked as xx(y)zz, with “xx” and “zz” respectively giving the amount of fuel injected in the first pilot or second main injection phase. While “y” represents the angle of rotation of the crankshaft between the pilot and the main injection. Fuel quantities are expressed as percentages of the total amount of fuel injected into the cylinder per process.

The results obtained by computer simulation are presented and compared with the “basic” motor in the form of a diagram.

Figure 14 shows the heat release rate curves for the nine fuel injection schemes (Schemes 1–9) while Figure 15 shows the effect of split injection on the pressure in the cylinder during the high-pressure part of the process. Both figures are showing curves for 75% of MCR power and the shape of curves obtained for 50% and 100% are very similar.

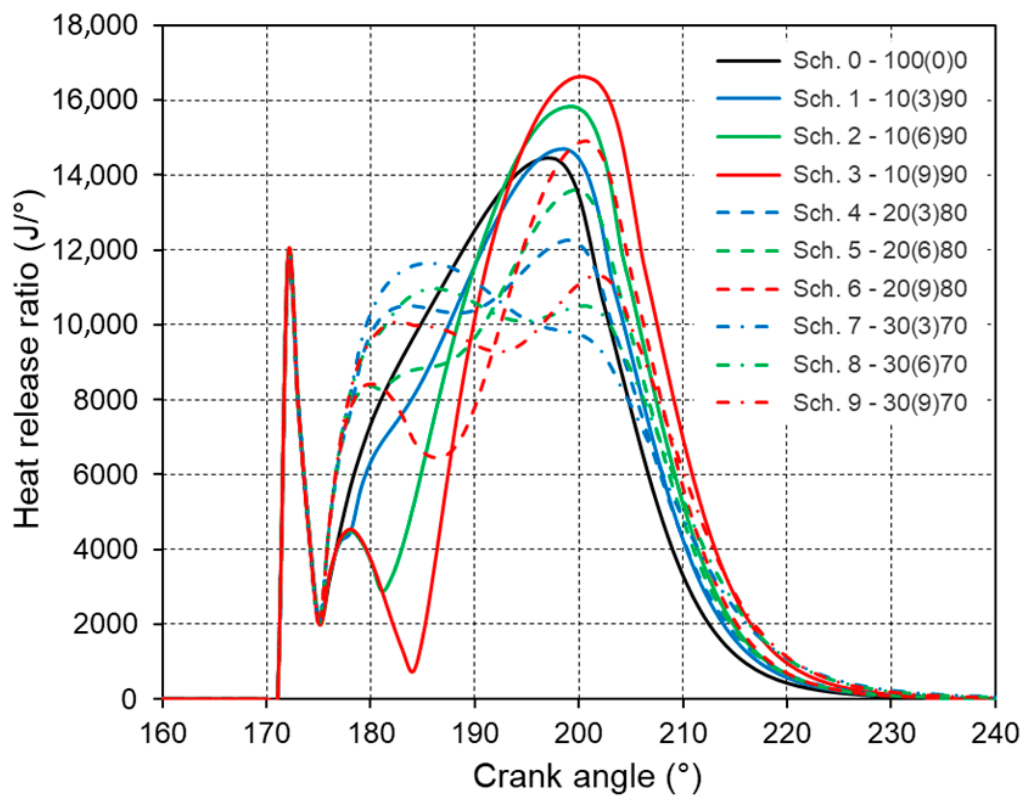


Figure 14. Influence of split injection on heat release at 75% of MCR power.

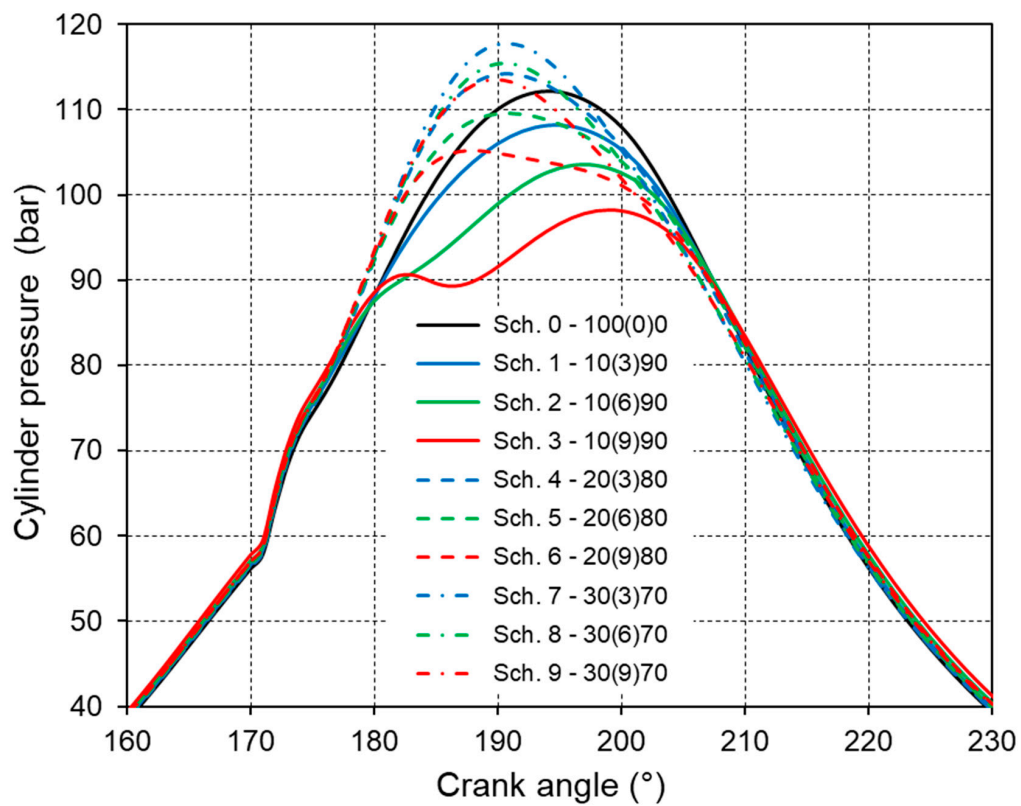


Figure 15. Influence of split injection on cylinder pressure at 75% of maximum continuous rating (MCR) power.

The diagrams shown in Figure 14 and the corresponding heat release rate curves show that split combustion consisting of “pilot” and “main” injection results in a reduction in heat release rate in the first part of the mixing controlled combustion phase whose intensity is determined by the rate of fuel mixture formation. In this case, a greater reduction in the rate of heat release in the first part of the mixing controlled combustion phase occurs with an increase in the difference $\Delta\varphi_{MI}$ between injections. As the proportion of injected “pilot” fuel increases, the effect on reducing the heat release rate decreases in the first part of the mixing controlled combustion phase but increases in the second part. The impact of split fuel injection on cylinder pressure is shown in Figure 15. There is a noticeable trend of decreasing cylinder pressure with increasing the difference $\Delta\varphi_{MI}$ between “pilot” and “main” injection. While increasing the amount of “pilot” fuel leads to a decrease in this effect. Further increase in the amount of “pilot” fuel also leads to an increase in the maximum pressure in the cylinder.

The effects of different nine split fuel injection schemes (Sch. 1 to 9) on SFOC, NO_x emission and maximum cylinder pressure at different engine loads compared to the base engine are shown in Figures 16–18.

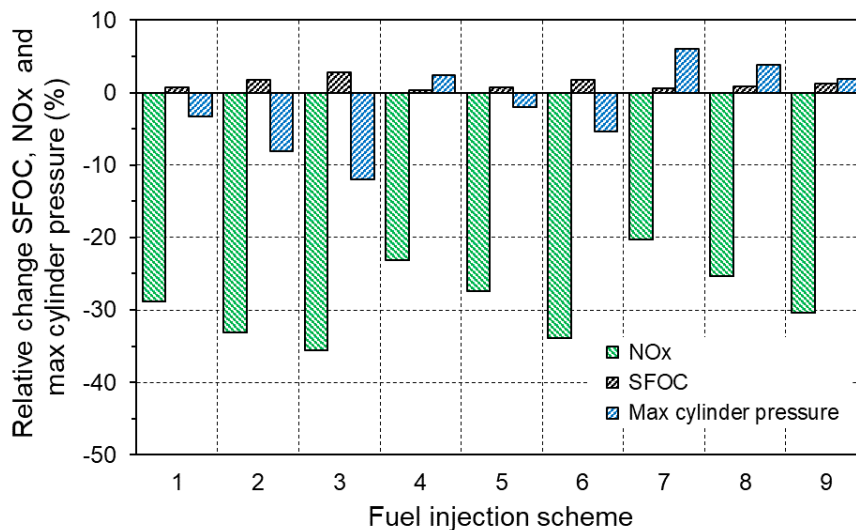


Figure 16. Influence of injection scheme on NO_x, specific fuel oil consumption (SFOC) and max cylinder pressure at 50% of MCR.

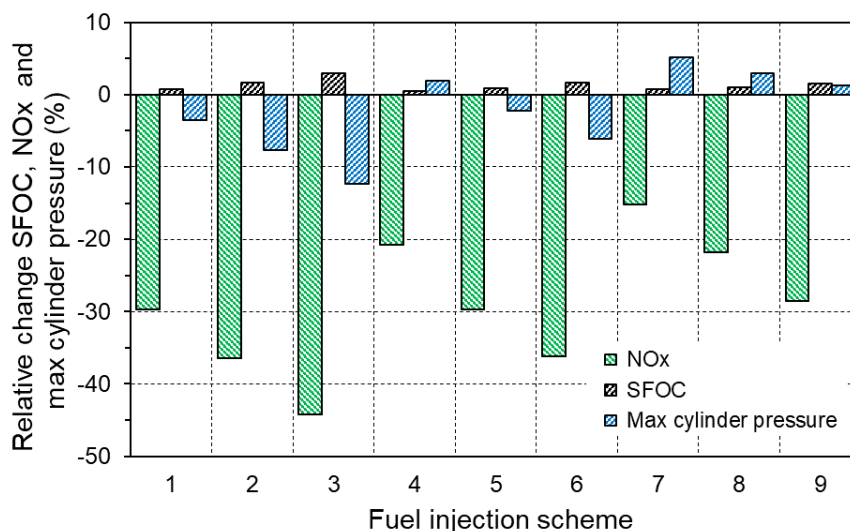


Figure 17. Influence of injection scheme on NO_x, SFOC and max cylinder pressure at 75% of MCR.

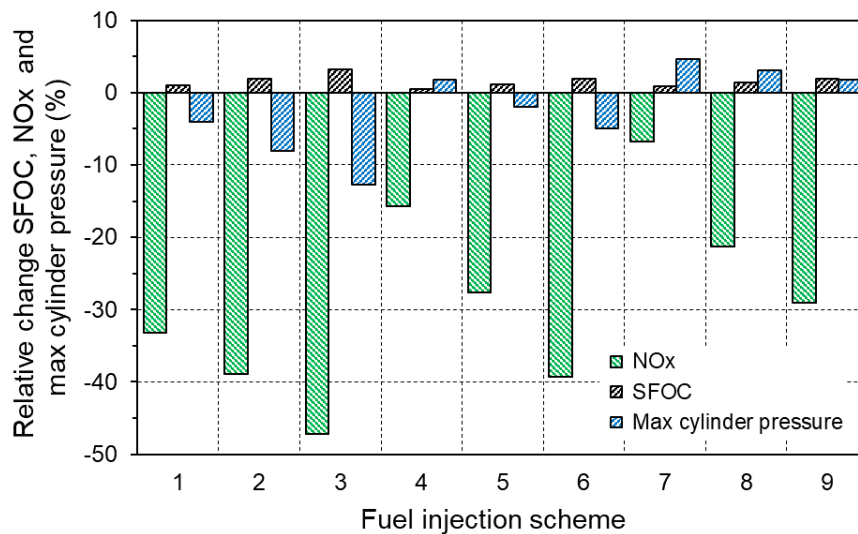


Figure 18. Influence of injection scheme on NO_x, SFOC and max cylinder pressure at 100% of MCR.

7. Conclusions

Marine propulsion systems are required to be as energy efficient as possible and to meet environmental protection standards. This paper analyzes the impact of split injection on fuel consumption and NO_x emissions of marine medium-speed diesel engines.

For the needs of the research, a zero-dimensional, two-zone numerical model of a diesel engine was developed. Comparison of the results obtained by the simulation with the available data of the engine manufacturer and from sea trials showed relatively small deviations of the numerical model in relation to the real engine. Sub-model based on the extended Zeldovich mechanism was applied to predict NO_x emissions.

The operation of the motor that drives synchronous generator was simulated under stationary conditions for three operating points and nine injection schemes. The results obtained by numerical simulations of engine operation indicate that by using split injection it is possible to achieve a relatively large reduction in NO_x emissions. However, all analyzed split injection schemes lead to increases in SFOC. Depending on the engine load, the NO_x emission is reduced from approximately 29% to 33% and the increase in fuel consumption specificity does not exceed 1%. It is possible to achieve greater reductions in NO_x emissions but with significant reductions in engine efficiency. The results are showing that NO_x emission reduction of up to 46% is achievable. However, this increases SFOC by approximately 3%. When increasing the angle between injection the maximum pressure decreases, so the amount of pilot injection is increased to compensate the difference.

Based on the results obtained by numerical simulations of engine operation, it is to be concluded that properly applied split fuel injection is an effective method for reducing NO_x emissions. If the appropriate scheme is applied it can be done without significant reduction in engine efficiency.

To continue research in this field an appropriate algorithm is to be developed since there are unlimited number of schemes that can be simulated and designed. Such an algorithm would allow faster and more accurate determination of the optimal injection scheme depending on the operating conditions of the engine.

Author Contributions: Formal analysis, R.R. and M.V.; Funding acquisition, M.V.; Investigation, V.P., T.M. and R.R.; Resources, M.V.; Software, V.P.; Validation, V.P. and T.M.; Writing—original draft, V.P.; Writing—review & editing, T.M. and R.R. All authors have read and agreed to the published version of the manuscript.

Funding: This work was partially supported by the Croatian Science Foundation under the project IP-2018-01-3739. This work was also supported by the University of Rijeka (project no. uniri-tehnic-18-18 1146 and uniri-tehnic-18-266 6469).

Conflicts of Interest: The authors declare no conflict of interest.

References

1. IMO-International Maritime Organization. Nitrogen Oxides (NO_x)-Regulation 13. Available online: [http://www.imo.org/en/OurWork/Environment/PollutionPrevention/AirPollution/Pages/Nitrogen-oxides-\(NOx\)-%E2%80%93-Regulation-13.aspx](http://www.imo.org/en/OurWork/Environment/PollutionPrevention/AirPollution/Pages/Nitrogen-oxides-(NOx)-%E2%80%93-Regulation-13.aspx) (accessed on 1 September 2020).
2. Wik, C. Reducing medium-speed engine emissions. *J. Mar. Eng. Technol.* **2010**, *9*, 37–44. [[CrossRef](#)]
3. Grimmeliuss, H.; Mesbahi, E.; Schulten, P.; Stapersma, D. The use of diesel engine simulation models in ship propulsion plant design and operation. In Proceedings of the 25th CIMAC World Congress, Wien, Austria, 21–24 May 2007; p. 227.
4. Heywood, J.B.; Sher, E. *The Two-Stroke Cycle Engine*; Taylor & Francis: London, UK, 1999.
5. Sorenson, S.C. *Engine Principles and Vehicles*; Technical University of Denmark: Lyngby, Denmark, 2008.
6. Mrakovčić, T. Osnivanje i Vođenje Brodskog Pogonskog Postrojenja Primjenom Numeričke Simulacije. Ph.D. Thesis, Faculty of Engineering, University of Rijeka, Rijeka, Croatia, 2003.
7. Račić, N. Simulacija Rada Brodskog Propulzijskog Sustava sa Sporohodnim Dizelskim Motorom u Otežanim Uvjetima. Ph.D. Thesis, Faculty of Engineering, University of Rijeka, Rijeka, Croatia, 2008.
8. Asay, R.J.; Svensson, K.I.; Tree, D.R. *An Empirical, Mixing-Limited, Zero-Dimensional Model for Diesel Combustion*; 2004-01-0924; SAE Technical Paper: Warrendale, PA, USA, 2004. [[CrossRef](#)]
9. Tauzia, X.; Maiboom, A.; Chesse, P.; Thouvenel, N. A new phenomenological heat release model for thermodynamical simulation of modern turbocharged heavy duty. *Diesel Engines* **2006**, *26*, 1851–1857. [[CrossRef](#)]
10. Descieux, D.; Feidt, M. One zone thermodynamic model simulation of an ignition compression engine. *Appl. Therm. Eng.* **2007**, *27*, 1457–1466. [[CrossRef](#)]
11. Jung, D.; Assanis, D.A. *Multi-Zone DI Diesel Spray Combustion Model for Cycle Simulation Studies of Engine Performance and Emissions*; 2001-01-1246; SAE Technical Paper: Warrendale, PA, USA, 2001. [[CrossRef](#)]
12. Kulkarni, A.M.; Shaver, G.M.; Popuri, S.S.; Frazier, T.R.; Stanton, D.W. Computationally efficient whole-engine model of a Cummins 2007 turbocharged diesel engine. *J. Eng. Gas Turbines Power* **2010**, *132*. [[CrossRef](#)]
13. Andersson, M.; Johansson, B.; Hultquist, A.; Nöhre, C. *A Real Time NO_x Model for Conventional and Partially Premixed Diesel Combustion*; 2006-01-0195; SAE Technical Paper: Warrendale, PA, USA, 2006. [[CrossRef](#)]
14. Maiboom, A.; Tauzia, X.; Shah, S.R.; Hetet, J.F. New phenomenological six-zone combustion model for direct injection diesel engines. *Energy Fuels* **2009**, *23*, 690–703. [[CrossRef](#)]
15. Durgun, O.; Sahin, Z. Theoretical investigation on heat balance in DI diesel engines for neat diesel fuel and gasoline fumigation. *Energy Convers. Manag.* **2009**, *50*, 43–51. [[CrossRef](#)]
16. Škifić, N. Analiza Utjecajnih Parametara Opreme na Značajke Dizelskog Motora. Ph.D. Thesis, University of Rijeka, Rijeka, Croatia, 2003.
17. Rakopoulos, C.D.; Rakopoulos, D.C.; Kyritsis, D.C. Development and validation of a comprehensive two-zone model for combustion and emissions formation in a DI diesel engine. *Int. J. Energy Res.* **2003**, *27*, 1221–1249. [[CrossRef](#)]
18. Kuleshov, A.S. *Use of Multi-Zone DI Diesel Spray Combustion Model for Simulation and Optimization of Performance and Emissions of Engines with Multiple Injection*; 2006-01-1385; SAE Technical Paper: Warrendale, PA, USA, 2006. [[CrossRef](#)]
19. Scappin, F.; Stefansson, H.S.; Haglund, F.; Andreasen, A.; Larsen, U. Validation of a zero-dimensional model for prediction of NO_x and engine performance for electronically controlled marine two-stroke diesel engines. *Appl. Therm. Eng.* **2012**, *37*, 344–352. [[CrossRef](#)]
20. Jafarmadar, S. The Effect of Split Injection on the Combustion and Emissions in DI and IDI Diesel Engines. In *Diesel Engine-Combustion, Emissions and Condition Monitoring*; Bari, S., Ed.; InTech: Rijeka, Croatia, 2013.
21. Juntarakod, P.; Soontornchainaksaeng, T. A Quasi-dimensional Three-zone Combustion Model of the Diesel Engine to Calculate Performances and Emission Using the Diesel-Ethanol Dual Fuel. *Contemp. Eng. Sci.* **2014**, *7*, 19–37. [[CrossRef](#)]
22. Finesso, R.; Spessa, E. A real time zero-dimensional diagnostic model for the calculation of in-cylinder temperatures, HRR and nitrogen oxides in diesel engines. *Energy Convers. Manag.* **2014**, *79*, 498–510. [[CrossRef](#)]

23. Baldi, F.; Theotokatos, G.; Andersson, K. Development of a combined mean value-zero dimensional model and application for a large marine four-stroke Diesel engine simulation. *Appl. Energy* **2015**, *154*, 402–415. [[CrossRef](#)]
24. Sindhu, R.; Amba Prasad Rao, G.; Madhu, M.K. Effective reduction of NO_x emissions from diesel engine using split injections. *Alex. Eng. J.* **2018**, *57*, 1379–1392. [[CrossRef](#)]
25. Savva, N.S.; Hountalas, D.T. Evaluation of a Semiempirical, Zero-Dimensional, Multizone Model to Predict Nitric Oxide Emissions in DI Diesel Engines' Combustion Chamber. *J. Combust.* **2016**, *2016*, 6202438. [[CrossRef](#)]
26. Sharma, S.; Sun, Y.; Vernham, B. Predictive Semi-Empirical NO_x Model for Diesel Engine. *Int. J. Energy Power Eng.* **2019**, *13*, 365–376. [[CrossRef](#)]
27. Medica, V. Simulation of Turbocharged Diesel Engine Driving Electrical Generator under Dynamic Working Conditions. Ph.D. Thesis, Faculty of Engineering, University of Rijeka, Rijeka, Croatia, 1988.
28. Pelić, V.; Mrakovčić, T.; Bukovac, O.; Valčić, M. Development and validation of 4 stroke diesel engine numerical model. *Pomor. Zb.* **2020**, *Special Edition*, 359–372.
29. Woschni, G. Die Berechnung der Wandwärmeverluste und der thermischen Belastung der Bauteile von Dieselmotoren. *MTZ-Mot. Z.* **1970**, *31*, 491–499.
30. Jankov, R. *Matematičko Modeliranje Strujno-Termodinamičkih Procesu i Pogonskih Karakteristika Dizel-Motora, I i II Dio*, 1st ed.; Naučna Knjiga: Beograd, Serbia, 1984.
31. Pflaum, W.; Mollenhauer, K. *Wärmeübergang in der Verbrennungskraftmaschine*, 1st ed.; Springer: Vienna, Austria, 1977; Volume 3. [[CrossRef](#)]
32. Löhner, K.; Döhring, E.; Chore, G. Temperaturschwingungen an der Innenwand von Verbrennungskraftmaschinen. *MTZ-Mot. Z.* **1956**, *12*, 413–418.
33. Hohenberg, G.F. *Advanced Approaches for Heat Transfer Calculations*; SAE Technical Papers: Warrendale, PA, USA, 1979. [[CrossRef](#)]
34. Heywood, J.B. Engine Combustion Modelling-An Overview. In *Combustion Modelling in Reciprocating Engines*; Plenum Press: New York, NY, USA, 1980; pp. 1–35.
35. Boulochos, K.; Papadopoulos, S. Zur Modellbildung des motorischen Verbrennungsablaufes. *MTZ-Mot. Z.* **1984**, *45*, 21–26.
36. Vibe, I.I. *Brennverlauf und Kreisprozess von Verbrennungsmotoren*; Verlag Technik: Berlin, Germany, 1970.
37. Woschni, G.; Anisits, F. Eine Methode zur Vorausberechnung der Änderung des Brennverlaufs mittelschnellaufender Dieselmotoren bei geänderten Betriebsbedingungen. *MTZ-Mot. Z.* **1973**, *34*, 106–115.
38. Betz, A.; Woschni, G. Umsetzungsgrad und Brennverlauf aufgeladener Dieselmotoren im instationären Betrieb. *MTZ-Mot. Z.* **1986**, *47*, 263–267.
39. Sitkei, G. Über den dieselmotorischen Zündverzug. *MTZ-Mot. Z.* **1963**, *26*, 190–194.
40. Boy, P. Beitrag zur Berechnung des Instationären Betriebsverhaltens von Mittelschnellaufenden Schiffsdieselmotoren. Ph.D. Thesis, Universität Hannover, Hannover, Germany, 1980.
41. Chapman, K. *Engine Airflow Algorithm Prediction, Introduction to Internal Combustion Engines*; Kansas State University: Manhattan, KS, USA, 2001. [[CrossRef](#)]
42. Bošnjaković, F. *Nauka o Toplini II.*; Tehnička Knjiga: Zagreb, Croatia, 1976.
43. Maass, H.; Klier, H. *Kräfte, Momente und Deren Ausgleich in der Verbrennungskraftmaschine*; Springer: Vienna, Austria, 1981. [[CrossRef](#)]
44. Hohlbaum, B. Beitrag zur Rechnerischen Untersuchung der Stickstoffoxid-Bildung Schellaufender Hohleistungsdieselmotoren. Ph.D. Thesis, Universität Fridricijana Karlsruhe, Karlsruhe, Germany, 1992.
45. Heider, G.; Woschni, G.; Zeilinger, K. 2-Zonen Rechenmodell zur Vorausberechnung der NO-Emission von Dieselmotoren. *MTZ-Mot. Z.* **1998**, *59*, 770–775. [[CrossRef](#)]
46. Provataris, S.A.; Savva, N.S.; Chountalas, T.D.; Hountalas, D.T. Prediction of NO_x emissions for high speed DI Diesel engines using a semi-empirical, two-zone model. *Energy Convers. Manag.* **2017**, *153*, 659–670. [[CrossRef](#)]
47. Weisser, G.A. Modelling of Combustion and Nitric Oxide Formation for Medium-Speed DI Diesel Engines: A Comparative Evaluation of Zero- and Three-Dimensional Approaches. Ph.D. Thesis, Universität Fridricijana Karlsruhe, Karlsruhe, Germany, 2001.

48. Rakopoulos, C.D.; Hountalas, D.T.; Tzanos, E.I.; Taklis, G.N. A fast algorithm for calculating the composition of diesel combustion products using 11 species chemical equilibrium scheme. *Adv. Eng. Softw.* **1994**, *19*, 109–119. [[CrossRef](#)]
49. *Wärtsilä 50DF-Product Guide*; Wärtsilä, Marine Solutions: Vaasa, Finland, 2019.
50. Nehmer, D.A.; Reitz, R.D. Measurement of the Effect of Injection Rate and Split Injections on Diesel Engine Soot and NO_x Emissions. In Proceedings of the SAE International Conference, Detroit, MI, USA, 28 February–3 March 1994.
51. Pierpont, D.A.; Montgomery, D.T.; Reitz, R.D. Reducing Particulate and NO_x Using Multiple Injections and EGR in a D.I. Diesel. In Proceedings of the SAE International Conference, Detroit, MI, USA, 27 February–2 March 1995.
52. Han, Z.; Uludogan, A.; Hampson, G.J.; Reitz, R.D. Mechanism of Soot and NO_x Emission Reduction Using Multiple-injection in a Diesel Engine. In Proceedings of the SAE International Conference, Detroit, MI, USA, 26–29 February 1996.

Publisher’s Note: MDPI stays neutral with regard to jurisdictional claims in published maps and institutional affiliations.



© 2020 by the authors. Licensee MDPI, Basel, Switzerland. This article is an open access article distributed under the terms and conditions of the Creative Commons Attribution (CC BY) license (<http://creativecommons.org/licenses/by/4.0/>).